

3-Phosphoinositide-dependent Kinase 1 Deficiency Perturbs Toll-like Receptor Signaling Events and Actin Cytoskeleton Dynamics in Dendritic Cells^{*[5]}

Received for publication, September 27, 2007, and in revised form, November 1, 2007 Published, JBC Papers in Press, November 8, 2007, DOI 10.1074/jbc.M708069200

Rossana Zaru, Pamela Mollahan, and Colin Watts¹

From the Division of Cell Biology and Immunology, Wellcome Trust Biocentre, University of Dundee, Dundee DD1 5EH, United Kingdom

The adaptive immune response depends on dendritic cell (DC) activation by microbial products that signal via pattern recognition receptors and activate mitogen-activated protein kinases, NF κ B and PI3K. The contribution of the AGC kinase family, including protein kinase B, protein kinase C, p90kDa ribosomal S6 kinase, and S6 kinase, has been little investigated because the probable redundancy among their isoforms makes their study difficult. We took advantage of the fact that all these kinases are regulated by the upstream master kinase 3-phosphoinositide-dependent kinase 1 (PDK1). Here we analyze various properties of DC from mice expressing ~10% of normal PDK1 (PDK1^{fl/-}). DC populations in lymphoid and nonlymphoid tissues appeared normal in PDK1^{fl/-} mice, and some *in vitro* responses to lipopolysaccharide (LPS) such as cytokine production were normal in cultured bone marrow DC. However, LPS-induced expression of class II major histocompatibility complex and CD86 were elevated in PDK1^{fl/-} BMDC and PDK1^{fl/-} spleen DC produced more interleukin-10 and -12, implying an attenuating role for PDK1. Unexpectedly, PDK1^{fl/-} DC had a significantly reduced capacity for LPS-stimulated macropinocytosis and phagocytosis that correlated with a lowered F-actin/G-actin ratio, apparently because of increased actin depolymerization. Several PDK1-regulated kinases, some of which feed into actin regulators, showed reduced activation in PDK1^{fl/-} DC. Reintroduction of PDK1 restored S6 kinase activity, increased levels of F-actin, and boosted macropinocytosis thus linking PDK1 and its downstream effectors to the unusual phenotype of PDK1^{fl/-} DC.

In dendritic cells (DC),² the recognition of pathogen-derived products induces a maturation program that will enable them, by presenting antigen to T lymphocytes, to initiate the adaptive

immune response. This crucial process involves a transient increase in antigen uptake and processing, the production of cytokines, the migration from the site of infection to the secondary lymphoid organs, antigen presentation, and up-regulation of class II MHC, as well as co-stimulatory molecules such as CD40 and CD86/80 (1–4). These events are regulated by complex signaling pathways downstream of pattern recognition receptors, such as Toll-like receptors (TLR). Whereas the role of mitogen-activated protein kinases, NF κ B, and interferon regulatory factors (IRFs) in regulating the different aspects of DC maturation, especially cytokine production, is under investigation (5, 6), there is still little information on the function of the Ser/Thr AGC kinases in DC activation by TLRs.

The Ser/Thr AGC family of protein kinases contains more than 50 members including enzymes such as Akt/PKB and PKC (7, 8). Studies performed in macrophages, neutrophils, and T and B lymphocytes showed that these kinases, once activated by extracellular stimuli, control a broad range of processes such as cell survival, gene transcription, migration, actin cytoskeleton rearrangement, and phagocytosis (reviewed in Ref. 8–15). In DC, most of these processes are modulated by TLR signaling (3–6, 16–19), but to date, the role of AGC kinases has been investigated only in the context of cytokine production. For instance, PKC ϵ has been shown to regulate IL-12 production (20), whereas GSK3, a downstream effector of Akt/PKB, controlled the balance between pro- and anti-inflammatory cytokines (21, 22).

One difficulty in studying AGC Ser/Thr kinases is the presence of many different isoforms, for instance there are 11 PKC isoforms (23) and three PKB isoforms (8). Therefore, deletion or inhibition of a single isoform could miss or underestimate the role of a particular kinase. To circumvent this problem, we took advantage of the fact that several members of the AGC kinases such as PKB, PKC, PRK1, RSK, S6K, and SGK require an upstream activatory “master” kinase, named PDK1 (7). Therefore, by manipulating PDK1 expression, we were able to have a more general view of the role of AGC kinases in DC functions.

Phosphoinositide-dependent protein kinase-1 (PDK1) is itself a member of the AGC kinase family and consists of a

^{*} This work was supported by a Medical Research Council Programme grant (to C. W.). The costs of publication of this article were defrayed in part by the payment of page charges. This article must therefore be hereby marked “advertisement” in accordance with 18 U.S.C. Section 1734 solely to indicate this fact.

^[5] The on-line version of this article (available at <http://www.jbc.org>) contains supplemental Figs. S1–S3.

¹ To whom correspondence should be addressed: Division of Cell Biology and Immunology, Wellcome Trust Biocentre, University of Dundee, Dow St., Dundee DD1 5EH, UK. Tel.: 44-1382-384233; Fax: 44-1382-385783; E-mail: c.watts@dundee.ac.uk.

² The abbreviations used are: DC, dendritic cell(s); PDK1, 3-phosphoinositide-dependent kinase 1; PKB, protein kinase B; RSK, p90kDa ribosomal S6 kinase; S6K, S6 kinase; GSK3, glycogen synthase kinase 3; APC, allophycocyanin; CFSE, carboxyfluorescein succinimidyl ester; PtdIns(3,4)P₂, phosphatidylinositol (3,4) biphosphate; PtdIns(3,4,5)P₃, phosphatidylinositol (3,4,5) triphosphate; SDC, spleen dendritic cells; BMDC, bone marrow-

derived dendritic cell(s); PKC, protein kinase C; LPS, lipopolysaccharide; MHC, major histocompatibility complex; IL, interleukin; TLR, Toll-like receptor(s); PH, pleckstrin homology; TTFC, tetanus toxin C-fragment; FACS, fluorescence-activated cell sorter; PE, phosphatidylethanolamine; FITC, fluorescein isothiocyanate; PBS, phosphate-buffered saline; TRITC, tetramethylrhodamine isothiocyanate; RBC, red blood cell(s); MFI, median fluorescent value; Ab, antibody; Erk, extracellular signal-regulated kinase; PI, phosphatidylinositol.

kinase domain, a hydrophobic pocket (known as the PDK1-interacting fragment (PIF) pocket) involved in substrate recognition, and a PH domain specific for phosphatidylinositol (3,4,5) triphosphate (PtdIns(3,4,5)P₃) and phosphatidylinositol (3,4) biphosphate (PtdIns(3,4)P₂) (24, 25). PDK1 activates its target kinases through the phosphorylation of their T loop. Under basal conditions, PDK1 exists in an active, phosphorylated form. Because this characteristic could result in a noncontrolled activation of the substrates, PDK1 recognizes its targets only when they are phosphorylated at a Ser/Thr residue in a hydrophobic motif. This preactivation step is achieved by stimulation with extracellular agonists. For example, PKB requires prior phosphorylation by mTor/riCTOR together with its binding to PtdIns(3,4,5)P₃ (26), whereas RSK isoforms need prior phosphorylation by Erk1/2 (27) to become activated by PDK1. In contrast with RSK and PKB, PKC isoforms are constitutive targets of PDK1. Indeed, phosphorylation by PDK1 stabilizes their conformation after synthesis (28, 29).

In the past few years, the crucial role of PDK1 in embryo development (30) as well as in the normal functions of the liver (31) and the heart (32) have been well studied using specific tissue deletion in mice. Recently, several studies have addressed the role of PDK1 in T lymphocytes. Hinton *et al.* (33) showed that, *in vivo*, PDK1 was required for the transition from the DN to the DP stages during thymocytes development. Using *in vitro* models, Nirula *et al.* (34) showed that PDK1 was involved in the production of IL-4 by Th2 cells. Here we investigate whether PDK1 and its AGC kinase substrates were involved in different aspects of DC behavior. To perform this study, we took advantage of the fact that although the loss of PDK1 is embryonic lethal, mice expressing only 10% of PDK1 activity are viable (30). The analysis of DC derived from these mice showed that despite normal development of DC *in vivo*, several aspects of their *in vitro* biology were disturbed. These included abnormal cytokine production by spleen-derived DCs and defects in both phagocytic function and TLR-induced macropinocytosis. The latter defects appeared to be due to reduced levels of polymerized actin in DC that could be due to the fact that several AGC kinase substrates of PDK1 are weakly activated by TLR stimuli. Our results have highlighted the importance of the fine tuning/balance of AGC kinase activity in controlling different aspects of DC biology.

EXPERIMENTAL PROCEDURES

Mice and Cell Culture—Wild type, PDK1^{+/fl} and PDK1^{-/-} mice in either C57BL/6 (backcrossed for at least five generations into C57BL/6) or in mixed C57BL/6 × Balb/c backgrounds were described previously (30). Briefly, the PDK1^{fl} allele in PDK1^{+/fl} and PDK1^{-/-} mice has a neomycin resistance gene in the intron between exons 2 and 3. This allele is not expressed effectively resulting in a 80–90% decrease of PDK1 expression in several PDK1^{fl/-} tissues (supplemental Fig. S1). For each experiment, age- and sex-matched wild type or PDK1^{+/fl} mice were used as littermate controls for PDK1^{-/-}. All of the mice were housed and maintained according to appropriate national and institutional guidelines. Dendritic cells were expanded from either mouse spleen (SDC) or bone marrow (BMDC) using complete RPMI supplemented with 10 ng/ml recombinant granulocyte macrophage-colony-stimulat-

ing factor (PeproTech) and 1 ng/ml transforming growth factor β (R & D Systems) or 10 ng/ml recombinant granulocyte macrophage-colony-stimulating factor, respectively, as described in Ref. 18. Unless otherwise stated, the experiments were performed in complete RPMI with 5% fetal calf serum without cytokines. The 5B12 T cell hybridoma specific for tetanus toxin C-fragment (TTFC) antigen was cultured as described in Ref. 35. CD4⁺ T cells specific for ovalbumin peptide 323–339 were purified using the CD4⁺ T cell isolation kit from Miltenyi (negative selection) from the spleen of OT-II mice (provided by P. Crocker, University of Dundee).

FACS Analysis of Surface Markers—Spleen, lymph nodes, and lungs were cut into pieces and digested in RPMI with 1 mg/ml collagenase A and 200 μg/ml DNase I (Roche) for 30 min at 37 °C. Tissues were disaggregated through a 70-μm filter, red blood cells were lysed, and the cells were co-stained with APC- or PE-labeled anti-CD11c and either PE-labeled anti-CD4, FITC-labeled anti-CD8, APC-labeled anti-CD11b, and PE-labeled anti-CD45RA (BD Biosciences), and the fluorescence was analyzed on a FACS Calibur (BD Biosciences). The epidermal sheets were prepared from ears. The ears were split in two, and each half was incubated for 1 h in PBS with 20 mM EDTA at 37 °C to allow the separation of the epidermis from the dermis. Epidermal sheets were fixed in 4% paraformaldehyde for 30 min and then blocked with 1% bovine serum albumin for 30 min. The sheets were permeabilized with 0.3% Triton X-100 and then stained with anti-class II MHC (M5/114, ATCC) followed by Alexa 594 donkey anti-rat Ab (Molecular Probes). The images were collected on a LSM 510 microscope (Zeiss). To measure up-regulation of class II MHC and co-stimulatory molecules, DC were either untreated or stimulated for 24 h with 50 ng/ml LPS and then co-stained with APC-labeled anti-CD11c and either PE-labeled antibodies against CD40, CD86 or CD54 Abs (Southern Biotech) or anti-class II MHC Ab followed by PE labeled goat anti-rat IgG Abs (Southern Biotech). The fluorescence was analyzed by FACS.

Cytokine Production—Five × 10⁴ BMDC or SDC were either untreated or stimulated with 50 ng/ml LPS for 1, 3, 6, or 12 h at 37 °C in a 96-well plate. IL-6, tumor necrosis factor α, IL-10, IL-12, and IL-1β productions were measured by enzyme-linked immunosorbent assay using a cytokine 10-plex bead kit from BioSource according to the manufacturer's instructions (Invitrogen).

Microscopy and Flow Cytometry Staining of F- and G-Actin—The cells were fixed with 4% paraformaldehyde, stained with 0.5 μg/ml TRITC-phalloidin (Sigma), and analyzed on a LSM510 microscope as described in Ref. 18. For flow cytometry analysis of actin content, 2 × 10⁵ DC were plated in 48-well plate for 1 h at 37 °C. After fixation with 4% paraformaldehyde, the cells were stained with PE-labeled anti-CD11c Ab, then permeabilized with 0.2% Triton X-100, and stained with 5 μg/ml FITC-DNase I and phalloidin Alexa 633 (1:100) (Molecular Probes, Invitrogen). The G-actin/F-actin ratio was calculated using the median fluorescent intensity measured by FACS on the CD11c-positive cell population.

DC plated as above were treated with 2 μM latrunculin A (Calbiochem) for 20 min at 37 °C. After two washes with warm RPMI, the cells were incubated for 5, 15, and 30 min either in

complete RPMI or in fetal calf serum-free medium with or without calcium at 37 °C, then fixed, and stained with Alexa633-phalloidin as described above.

Dextran Uptake—Dextran uptake was performed as described previously (18). Briefly, 2×10^5 DC were either untreated or stimulated with 50 ng/ml LPS (Calbiochem), 5 μ g/ml CpG (OD1668, MWG), or 50 ng/ml Pam3CSK (EMC Microcollections) for the indicated period of time, and then 1 mg/ml FITC or (in the case of retrovirally infected, GFP-positive cells) Alexa 633 dextran (Invitrogen) was added for 10 min at 37 °C. The cells were washed four times at 4 °C with PBS/0.2% fetal calf serum, stained with APC- or PE-labeled anti-CD11c Abs, and analyzed by FACS. Note that Alexa 633-dextran bound to the cell surface to a greater extent than FITC-dextran partially masking LPS-stimulated endocytosis, which was reduced under these conditions to an apparent value of 1.5–2-fold in wild type cells and less in PDK1^{+/-} cells.

T Cell Assays—Wild type, PDK1^{+/-}, and PDK1^{-/-} BMDC or SDC (5×10^5) were pulsed with the indicated concentrations of either ovalbumin (Worthington Biochemical Corporation) or TTFC (35) for 40 min in presence of 50 ng/ml LPS. After three washes, 5×10^5 5B12 T cell hybridomas or OT-II T cells were added to a final volume of 200 μ l of complete RPMI in 96-well plates. After 24 h, the supernatants were collected, and the amount of IL-2 was measured by enzyme-linked immunosorbent assay using the IL-2 OptEIA kit (BD Biosciences). In other experiments, DC were stimulated for 24 h with 50 ng/ml LPS at 37 °C and then pulsed with TTFC peptide 900–915 (35) or ova peptide 323–339 (Bachem) for 3 h at 37 °C before the addition of T cells.

Red Blood Cell Phagocytosis—Sheep red blood cells (RBC, 10^8 cells) (Diagnostics Scotland) were opsonized with rabbit anti-sheep IgG (1:50; Harlan Sera-Lab) for 45 min at 37 °C in 500 μ l of RPMI-Hepes and then labeled with 0.5 μ M CFSE (Molecular Probes) for 15 min at 37 °C. RBC were washed with RPMI-Hepes once and added at a 40:1 ratio to 2.5×10^5 DC previously plated in 24-well plates. The plate was centrifuged for 1 min at $500 \times g$ at 37 °C and then cells incubated for 10 or 25 min at 37 °C. After two washes with RPMI, excess extracellular RBC were lysed in RBC lysis buffer (Sigma) for 1 min at room temperature, and then cells were washed again twice. DCs were harvested with 5 mM EDTA/PBS and stained at 4 °C with APC-labeled anti-CD11c Abs, and CFSE fluorescence reflecting RBC uptake DC was measured by FACS. The results are expressed either as median fluorescent value (MFI) or as the percentage of CD11c⁺ cells that are CFSE-positive. RBC phagocytosis was also assessed by microscopy after fixation and staining with TRITC-phalloidin as described above.

Cell Lysis and Immunoblot—SDC (10^6 cells) were either untreated or treated with 50 ng/ml LPS for 30 min at 37 °C in 6-well plates, harvested from the wells, and lysed in SDS sample buffer. Equal amounts of proteins (10–20 μ g) were loaded on SDS-PAGE gels, transferred to nitrocellulose, and immunoblotted with the following antibodies against: RSK2, Erk1/2, WASP (Santa Cruz Biotechnology), cofilin, PDK1 (Cell Signaling), Arp3 (kind gift of M. Welch, UC Berkeley, CA), and actin (ICN). Phospho-specific antibodies against RSK S227 (R & D Systems) and p42/44 (Erk1/2), p38, cofilin S3, PKB T308, and GSK3 α/β S9/21 were purchased from Cell Signaling. For some

experiments, secondary antibodies coupled to IRDye800 (LI-COR Biosciences) or to Alexa 680 (Molecular Probes) were used and detected by LI-COR Odyssey infrared detection system (Rockland). Band intensity was quantitated using LI-COR software.

Flow Cytometry Analysis of S6 Phosphorylation—PDK1^{fl/+} or PDK1^{fl/-} SDC or BMDC (2×10^5) were untreated or stimulated with 50 ng/ml LPS for 30 min at 37 °C. The cells were stained on ice with APC-labeled anti-CD11c abs. After washing, the cells were fixed in 0.5% paraformaldehyde for 15 min at 37 °C and then permeabilized with 90% cold methanol on ice for 15 min. After blocking with 1% bovine serum albumin in PBS, the cells were stained with anti-phospho-S6 abs (Cell Signaling) followed by goat anti-Rabbit PE abs (Jackson ImmunoResearch) and then analyzed by FACS (33). The MFI was measured on CD11c⁺-gated cells.

[Ca²⁺]_i Measurement—SDC (2×10^5) were labeled with 5 μ M Indo-1 (Invitrogen) for 45 min at 37 °C and then washed. Calcium flux in DC was recorded for 2 min on a LSR machine (BD biosciences). After 30 s 100 ng/ml MIP1 α (Peprotech) was added. Emission was measured at 405 and 525 nm. The 405/525 ratio gives a measure of [Ca²⁺]_i increase in stimulated cells.

Retroviral Constructs and BMDC Retroviral Infection—Moloney murine leukemia virus-based pBMN-IRES-GFP retroviral vector was provided by G. Nolan (Stanford). Mouse PDK1 cDNA was isolated from pME18-FL3 vector (provided by D. Alessi, University of Dundee) and cloned into the EcoRI and NotI sites of pBMN-I-GFP by Advantagen Ltd., (Dundee, UK). The virus was produced by transfecting Phoenix Eco 293T packaging cell line as previously described in Ref. 18. Viral supernatant was concentrated five times in a Beckman centrifuge (rotor JA 25.50) at 20,000 $\times g$ at 4 °C for 4 h. BMDC were infected at days 2 and 3 with viral supernatant supplemented with 8 μ g/ml polybrene as described in Ref. 18. The cells were used after 8 days. GFP expression was assessed by flow cytometry. To assess PDK1 overexpression, BMDC were lysed, and equal amounts were loaded on a SDS-PAGE gel. After transfer, the nitrocellulose membrane was immunoblotted with anti-PDK1 Ab.

Statistical Analysis—Statistical significance was assessed by unpaired Student's *t* test. Differences with *p* values of <0.05 were considered statistically significant.

RESULTS

DC Development Appears Normal in PDK1^{-/-} Mice—PDK1^{-/-} mice carry an insertion of a neomycin cassette into the single functional PDK1 allele (fl), which results in the expression of ~10% of wild type levels of the enzyme (Fig. 1C, supplemental Fig. S1) (30). After backcrossing, PDK1^{-/-} mice were not born at the expected Mendelian ratio, indicating a more penetrating effect of the fl allele in the pure B6 background during embryonic development. Nonetheless, a limited number of mice were obtained for analysis. DC derived from both genetic backgrounds were used for all of the experiments, and the results were similar. We first investigated whether low levels of PDK1 expression could affect the development of DC *in vivo* as well as their homing to immune and

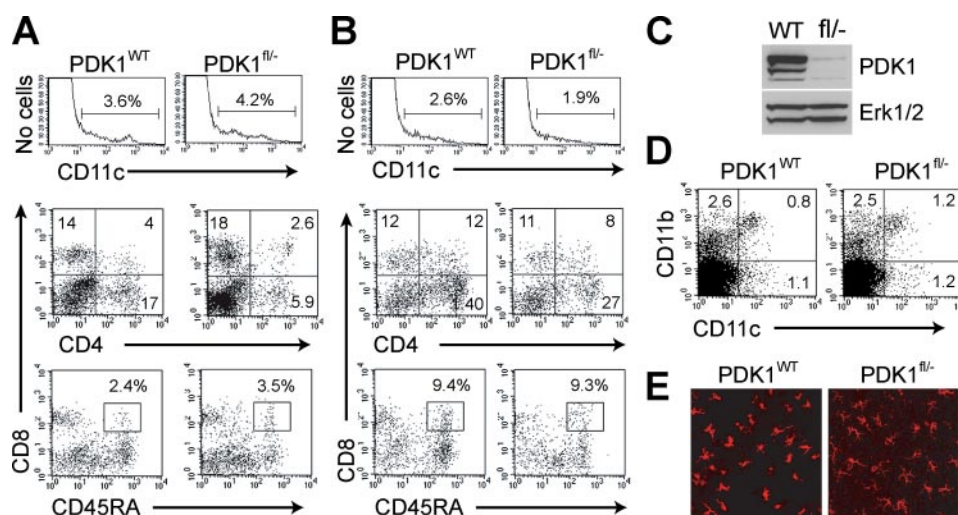


FIGURE 1. Analysis of DC populations ex vivo. Spleen (A) or lymph node (B) cells isolated from $PDK1^{+/+}$ or $PDK1^{fl/-}$ mice were co-stained with anti-CD11c, anti-CD4, anti-CD8, and anti-CD45RA Abs and analyzed by flow cytometry. The histograms (top) show the percentage of cells expressing CD11c. The upper dot plots show the expression pattern of CD4 and CD8 in CD11c⁺ cells, and the lower dot plots showed the expression pattern of CD8 and CD45RA in CD11c⁺ cells. The numbers in each plot correspond to the percentages of CD11c⁺ cells expressing the indicated marker combination. C, lysates were made from $PDK1^{+/+}$ and $PDK1^{fl/-}$ BMDCs, loaded on a SDS-PAGE gel, and immunoblotted with anti-PDK1 Ab and anti-Erk1/2 Ab as a loading control. D, lung cells isolated from $PDK1^{+/+}$ or $PDK1^{fl/-}$ mice were co-stained with anti-CD11c and anti-CD11b Abs and analyzed by flow cytometry. The numbers correspond to the percentage of total cells expressing the indicated marker combination. E, ear epidermal sheets from $PDK1^{+/+}$ or $PDK1^{fl/-}$ mice were fixed and then stained with anti-class II MHC Abs (red), and the fluorescence was analyzed by confocal microscopy. WT, wild type.

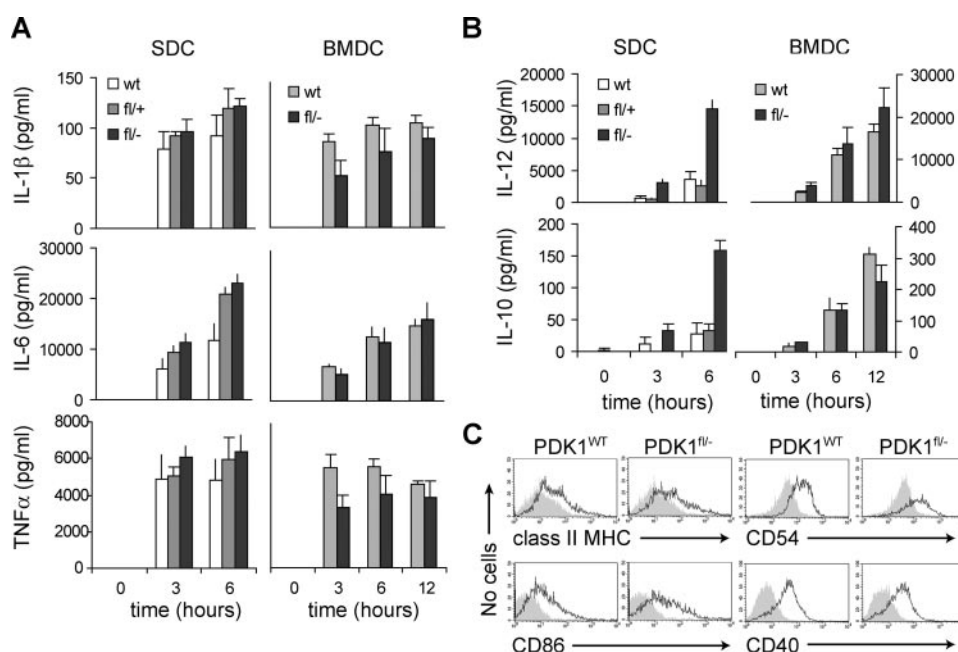


FIGURE 2. LPS induced long term maturation is normal in $PDK1^{-/-}$ DC. A and B, SDC (left panels) or BMDC (right panel) generated *in vitro* from $PDK1^{+/+}$, $PDK1^{fl/+}$, or $PDK1^{fl/-}$ mice were stimulated for the indicated time periods with 50 ng/ml LPS. Secretion of IL-6, tumor necrosis factor α , IL-10, IL-12, and IL-1 β was detected by enzyme-linked immunosorbent assay. C, BMDC generated *in vitro* from $PDK1^{+/+}$ or $PDK1^{fl/-}$ mice were either untreated or stimulated with 50 ng/ml LPS for 24 h at 37 °C, co-stained with anti-CD11c and either anti-CD40, anti-CD86, anti-CD54, or anti-class II MHC and analyzed by flow cytometry. Overlay histograms show the surface expression of class II MHC, CD86, CD54, or CD40 in CD11c⁺ cells either untreated (gray) or treated with LPS (white). The results are representative of three independent experiments. wt, wild type.

nonimmune tissues. We used CD11c as a general marker to identify DC populations. As shown in Fig. 1 (A and B), the percentage of CD11c⁺ cells in the spleen and in the lymph nodes of $PDK1^{-/-}$ mice was normal. Several DC subsets have been characterized based on their expression of CD4 and CD8

(conventional DC) or CD8 and CD45RA (plasmacytoid DC) (36, 37). Using different combinations of these markers, we found that the different subsets of CD11c⁺ DC were present in the spleen and in the lymph nodes, although in slightly altered proportions. In particular, fewer CD11c⁺CD4⁺ DC were detected in the spleen and lymph nodes of $PDK1^{-/-}$ mice (Fig. 1, A and B).

To perform their sentinel role in the immune system, DC have to populate nonlymphoid tissues. We therefore analyzed the presence of DC in the lungs and in the epidermis. Fig. 1D showed that in the lungs of $PDK1^{-/-}$ mice, CD11c⁺CD11b⁺ DC were present at the same levels as in the littermate control mice. To detect Langerhans cells, which are the DC that reside in the epidermis (37), epidermal ear sheets were stained with anti-class II MHC Abs. The results showed that $PDK1^{-/-}$ Langerhans cells were present at the same density, and their overall morphology was similar to wt Langerhans cells (Fig. 1E). Taken together the above results indicate that low levels of PDK1 activity affect neither the generation of DC from bone marrow precursors nor their homing to lymphoid and nonlymphoid organs.

Long Term Maturation Induced by TLR Is Not Affected by Reduced PDK1 Activity—To perform a more detailed analysis of DC functions we generated DC from either bone marrow (BMDC) or spleen (SDC) of $PDK1^{wt}$, $PDK1^{fl/+}$, and $PDK1^{-/-}$ mice *in vitro*. We assessed whether TLR-induced maturation required normal levels of PDK1 activity. We measured the production of several cytokines including IL-1 β , IL-10, IL-12, tumor necrosis factor α , and IL-6 at different time points after LPS stimulation either in BMDC or in SDC. As shown in Fig. 2A, the secretion of IL-1 β , tumor necrosis factor α and IL-6 by $PDK1^{-/-}$ SDC or BMDC proceed with similar kinetics as in the $PDK1^{wt}$ - or $PDK1^{fl/+}$ -derived DC. Interestingly, although production of IL-12 and IL-10 was not affected in $PDK1^{-/-}$ BMDC, in $PDK1^{-/-}$ SDC the levels of both cytokines were strongly increased (Fig. 2B). This result indi-

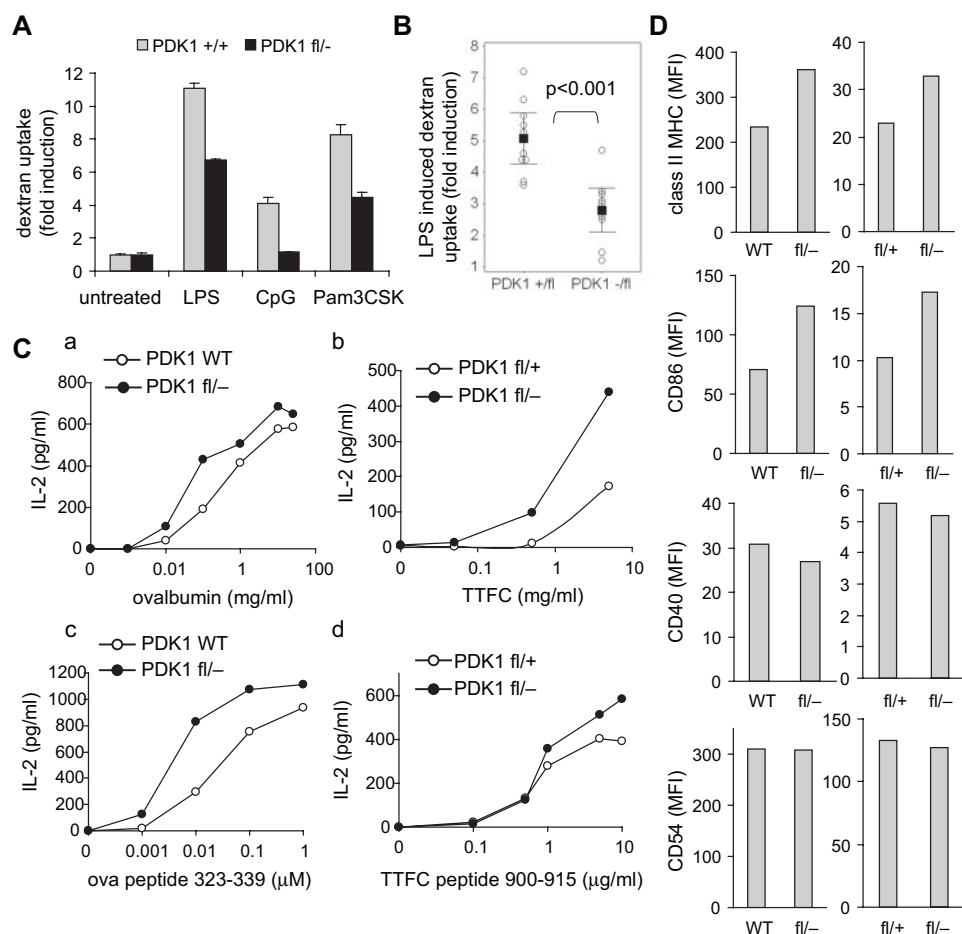


FIGURE 3. TLR-induced macropinocytosis is impaired in PDK1^{fl/fl} DC. *A*, left panel, wild type or PDK1^{fl/fl} BMDC were either untreated or stimulated with 50 ng/ml LPS, 10 μ g/ml CpG and 50 ng/ml Pam3CSK for 30 min followed by 10 min of incubation with 1 mg/ml FITC-dextran. Dextran uptake was assessed by flow cytometry. The results are expressed as fold induction (median intensity value) relative to FITC-dextran uptake in untreated cells. *B*, FITC-dextran uptake fold induction induced by LPS in DC derived from PDK1^{fl/+} or PDK1^{fl/fl} DC. The open circles correspond to single mice each ($n = 10$ for each genotype). The black square represents the mean. The bars represent 95% confidence interval. Reduced fold induction in PDK1^{fl/fl} DC was significant ($p < 0.0001$). *C*, IL-2 release by OT-II T cell (panels *a* and *c*) or 5B12 T cell hybridomas (panels *b* and *d*) incubated with either wild type (WT), PDK1^{fl/+}, or PDK1^{fl/fl} DC, which were pulsed with increasing amount of ovalbumin (panel *a*) or tetanus toxin C-fragment (TTFC, panel *b*) in presence of LPS or with DC pretreated with LPS for 24 h and then pulsed with increasing amount of ova peptide 323–339 (panel *c*) or TTFC peptide 900–915 (panel *d*) as described under “Experimental Procedures.” BMDC (panels *a* and *c*) or SDC (panels *b* and *d*) were used. The results are representative of three to four independent experiments performed in duplicate using BMDC and SDC derived from one littermate control and one PDK1^{fl/fl} mouse each time in either C57 or mixed backgrounds. *D*, BMDC (left panels) or SDC (right panels) derived from the same mice used in *B* were either stimulated with 50 ng/ml LPS for 24 h, co-stained with anti-CD11c and either anti-CD40, anti-CD86, anti-CD54, or anti-class II MHC, and analyzed by flow cytometry. The results are representative of three independent experiments performed in duplicate using BMDC and SDC derived from one littermate control and one PDK1^{fl/fl} mouse each time.

icates that low levels of PDK1 activity do not compromise the production of normal levels of cytokines in response to LPS stimulation, and in fact, PDK1 may act to constrain production of IL-12 and IL-10, at least in SDCs. Another important feature of TLR-induced DC maturation is the up-regulation of class II MHC and co-stimulatory molecules such as CD40, CD86, and CD54 (2). The cells were stained with antibodies against these different surface markers 24 h after LPS addition. FACS analysis showed that PDK1^{fl/fl} DC up-regulated class II MHC, CD40, CD86, and CD54 and in some cases to greater levels than wild type DC (Fig. 2C and see below).

TLR-induced Macropinocytosis Is Reduced in PDK1^{fl/fl} DCs—TLR signaling induces a variety of cellular responses in addition to *de novo* expression of cytokines and co-stimulatory mole-

cules. Previously, we showed that the initial stimulation of DC with TLR ligands induced a transient increase in actin-dependent macropinocytosis that peaks at 30–40 min after TLR stimulation (18). To monitor macropinocytosis, control DC or DC stimulated with different TLR ligands were incubated with FITC-dextran. We found that although the basal levels of dextran uptake were not affected (data not shown), the TLR-mediated increase was partially impaired (between 50 and 70%) in PDK1^{fl/fl} DCs stimulated with LPS, Pam3CSK, or poly(I-C) and completely abolished in the case of CpG addition (Fig. 3, *A* and *B*, and data not shown). The acute increase and the subsequent down-regulation of macropinocytosis in PDK1^{fl/fl} DCs followed the same kinetics as in control DCs, but the enhanced phase of uptake was reduced in PDK1^{fl/fl} DCs (supplemental Fig. S2A). To investigate whether the reduction in antigen uptake could result in impaired antigen presentation to T cells, we measured IL-2 secretion by T cells stimulated with control littermate or PDK1^{fl/fl} DCs pulsed with either ovalbumin or TTFC antigen in the presence of LPS. Surprisingly, the amount of IL-2 produced was higher in T cells stimulated by PDK1^{fl/fl} DCs (Fig. 3, *C*, panels *a* and *b*). We investigated the possibility that expression of co-stimulatory and/or class II MHC molecules on the surface of LPS-matured PDK1^{fl/fl} DCs was higher than on wild type DC, which might compensate for reduced antigen uptake.

Indeed, as shown in Fig. 3D, the amount of CD86 and class II MHC were higher in PDK1^{fl/fl} DCs compared with littermate control DC, although CD40 and CD54 expression were not increased in PDK1^{fl/fl} DC (Fig. 3D). To further confirm the effect of enhanced expression of these molecules, T cells were stimulated with peptide pulsed DC either fresh or fixed after peptide loading. As shown in Fig. 3C (panels *c* and *d*) and in supplemental Fig. S2B, IL-2 production was enhanced in T cells stimulated by PDK1^{fl/fl} DCs. Thus, LPS-matured DC with low PDK1 activity overcame their reduced capacity to uptake antigen by expressing higher levels of class II MHC and CD86 molecules at their surface.

FcR-mediated Phagocytosis Is Reduced in PDK1^{fl/fl} DCs—To gain further insight into the defect in actin-dependent endocy-

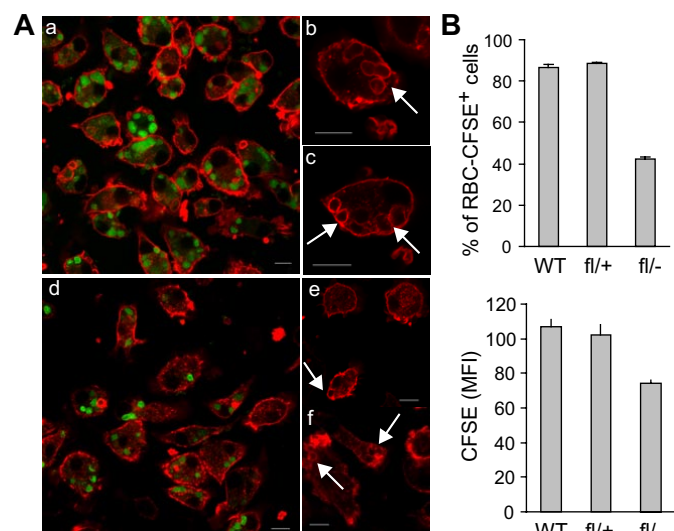


FIGURE 4. FcR-mediated phagocytosis is impaired in PDK1^{fl/fl} DC. CFSE-labeled RBC were incubated at a 40:1 ratio with SDC generated *in vitro* from PDK1^{+/+}, PDK1^{fl/+}, or PDK1^{fl/-} mice for either 10 (A, panels b, c, e, and f) or 25 min (A, panels a and d, and B) at 37 °C. RBC that have not been phagocytosed were lysed with RBC lysing buffer. A, cells were fixed and stained with phalloidin TRITC and analyzed by confocal microscopy. The arrows indicate phagocytic cups (panels a–c, wild type (WT); panels d–f, PDK1^{fl/-}). Bar, 10 μ m. B, CFSE-labeled RBC uptake was measured by flow cytometry. The results are expressed as the percentage of DC that have uptake RBC (top panel) or as the median intensity value (bottom panel). The results were performed in either SDC or BMDC and are representative of three independent experiments.

tosis, we asked whether phagocytosis, which requires the activation of several PDK1 substrates as well as a functional actin cytoskeleton, was also affected. To measure the capacity of PDK1^{fl/fl} DC to phagocytose, CFSE-labeled RBC were opsonized with rabbit anti-sheep IgG and incubated with DC for the indicated time periods. Phagocytosis was assessed by microscopy and by flow cytometry. As illustrated in Fig. 4B, after 25 min, only 40% of PDK1^{fl/fl} DC had phagocytosed RBC compared with almost 90% in littermate controls. Moreover, the number of RBC engulfed by these cells was reduced compared with littermate control DC (Fig. 4). An essential step of phagocytosis is the accumulation of a ring of F-actin at the site of the nascent phagocytic cup. As shown in Fig. 4A, PDK1^{fl/fl} DC had fewer F-actin rings compared with control DCs, suggesting that low PDK1 expression levels could affect the accumulation of F-actin at the phagocytic cup during FcR-mediated phagocytosis. Taken together these results indicate that two different actin-dependent modes of endocytosis, macropinocytosis and phagocytosis, are reduced in DC expressing low levels of PDK1.

F-actin Content Is Reduced in PDK1^{fl/fl} DCs—Phagocytosis and TLR-mediated macropinocytosis require a rapid mobilization of the actin cytoskeleton. The above data suggest that this may be defective when PDK1 levels are low. To investigate this hypothesis further, we first compared the morphology of PDK1^{wt}, PDK1^{+/+}, and PDK1^{fl/fl} DC by analyzing the distribution of F-actin. As shown in Fig. 5A, PDK1^{fl/fl} DC adhered to the glass substrate and spread to the same extent as control DCs. Although the typical F-actin based structures displayed by DC such as cortical actin, cables, focal adhesions, and podosomes were present in PDK1^{fl/fl} DC, we observed a striking reduction in the intensity of phalloidin staining, suggesting that

these cells had lower levels of F-actin. To obtain a more quantitative measurement for F-actin content, the cells were stained with phalloidin Alexa 633 to detect F-actin together with FITC-DNase I, which recognized G-actin as an internal control. The respective fluorescence were measured by FACS, and the G/F-actin ratio was calculated. The G/F-actin ratio was significantly higher in PDK1^{fl/fl} DC compared with PDK1^{wt} or PDK1^{+/+} DC (Fig. 5, B and C), consistent with the lower level of F-actin observed by microscopy.

One possible explanation for this reduction is that PDK1^{fl/fl} DC express less total actin. However, we found no significant alteration of actin levels in PDK1^{fl/fl} DC cell lysates (Fig. 5D). Another explanation could be that less G-actin monomers are available for polymerization (sequestration) or that the rate of actin polymerization is reduced in PDK1^{fl/fl} DCs. To test this possibility, the cells were treated with latrunculin A to depolymerize actin filaments. The drug was then removed, and the levels of F-actin were measured at different time points during the recovery phase. The results showed that the polymerization of F-actin proceeded more slowly in PDK1^{fl/fl} DC compared with littermate control DC (Fig. 5E). F-actin levels are determined by a balance between actin polymerization and depolymerization, both of which are regulated by actin-binding proteins. The two key proteins implicated in the initiation of actin polymerization are WASP and Arp2/3 (38, 39). Analysis of their levels of expression by Western blot showed equivalent amounts in PDK1^{fl/fl} DC relative to wild type (Fig. 5D), although it is possible that their activity is affected by the reduced activation of PDK1 substrates. Another actin-binding protein that is determinant for F-actin accumulation in cells is cofilin, which severs actin filaments (40). Its capacity to depolymerize F-actin is regulated by phosphorylation on Ser³, which decreases its activity. We found that phosphorylation of cofilin on Ser³ was reduced in PDK1^{fl/fl} DC compared with control DCs, suggesting that cofilin activity is higher in these cells (Fig. 5F). This result suggested that the slower rate of F-actin recovery observed in PDK1^{fl/fl} DC could result from an increased depolymerization activity of cofilin. To analyze whether actin polymerization could also be affected, the same experiment as in Fig. 5E was performed in the absence of calcium in the medium during the recovery phase after Lat A treatment. Conversely to polymerization, actin depolymerization requires calcium influx (41). Therefore, by removing calcium during the recovery phase, only polymerization will be monitored. Fig. 5G shows that in the absence of calcium, F-actin levels increased faster in both littermate and PDK1^{fl/fl} DC. Moreover, the recovery proceeded at the same speed in both DC, suggesting that low levels of PDK1 affected F-actin depolymerization but not F-actin polymerization. Finally, we also ruled out the possibility that low levels of PDK1 affected Ca²⁺ entry because calcium influx induced by the chemokine MIP1 α was normal in PDK1^{fl/fl} DC (Fig. 5H). Taken together, the reduced F/G-actin ratio may well explain the reduced macropinocytic and phagocytic response observed in PDK1^{fl/fl} DCs.

Reduced PDK1 Activity Induced a Decrease in RSK, PKB, and S6 Activation—The PDK1^{fl/fl} DC showed striking disturbances in disparate processes including actin cytoskeleton dynamics and regulation of cytokine expression. This suggested that dif-

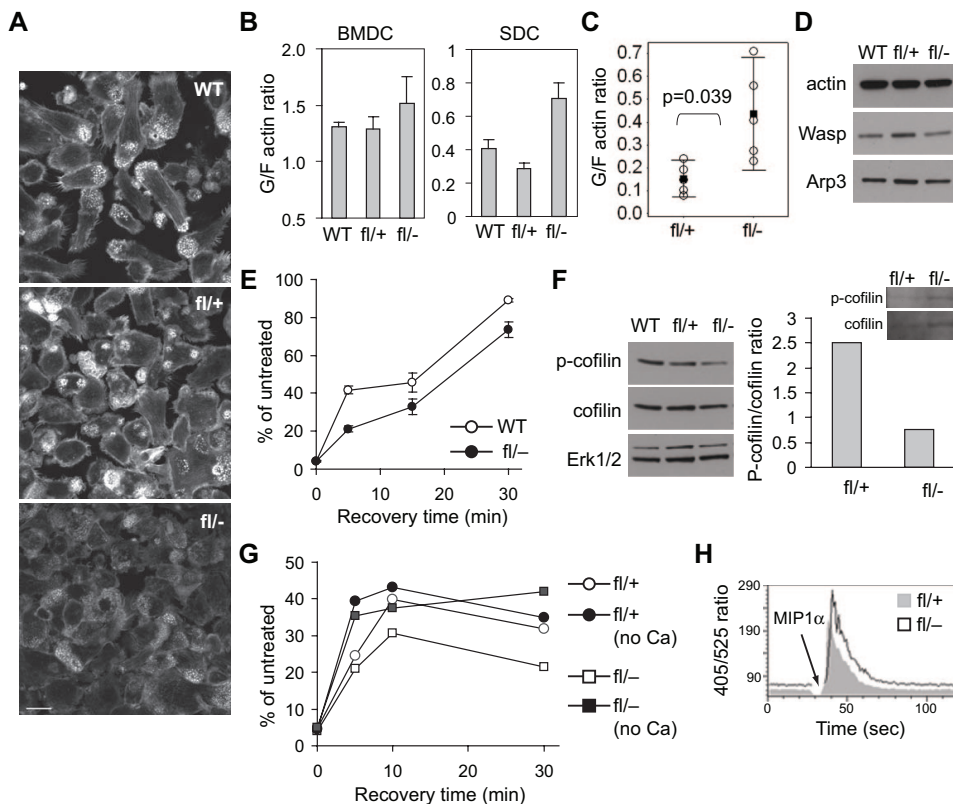


FIGURE 5. F-actin content and actin polymerization rate are reduced in DC with low PDK1 activity. A, PDK1^{+/+}, PDK1^{fl/+}, or PDK1^{fl/-} SDCs were stained with TRITC-phalloidin, and the fluorescence was analyzed by confocal microscopy. Bar, 20 μ m. B, PDK1^{+/+}, PDK1^{fl/+}, or PDK1^{fl/-} BMDC (left panel) or SDC (right panel) were co-stained with anti-CD11c Ab and FITC-DNase I (G-actin) and Alexa 633-phalloidin (F-actin). The respective fluorescence in CD11c⁺ cells were analyzed by flow cytometry. The G/F-actin ratio was calculated using median intensity values. The mean \pm S.D. of a representative experiment performed in triplicate is shown. C, G/F-actin ratio in PDK1^{fl/+} and PDK1^{fl/-} DC. The open circles correspond to one mouse each ($n = 6$ for each genotype). The black squares represent the means. The bars represent 95% confidence interval. The increased G/F-actin ratio in PDK1^{fl/-} DC was significant ($p = 0.039$). D, lysates of PDK1^{+/+}, PDK1^{fl/+}, or PDK1^{fl/-} SDCs were separated by SDS-PAGE and immunoblotted with anti-actin, anti-WASP or anti-Arp3 Abs. The results are representative of at least three independent experiments. E, PDK1^{fl/+} or PDK1^{fl/-} BMDC were untreated or treated with 2 μ M latrunculin A for 20 min at 37 $^{\circ}$ C, washed, and let recover for the indicated time periods before fixation. The cells were stained with anti-CD11c Ab and TRITC-phalloidin and analyzed by flow cytometry. The results are expressed as the % of F-actin content (median fluorescence value) in CD11c⁺ cells relative to untreated cells. The same results were obtained in either SDC or BMDC in three independent experiments. F, lysates of PDK1^{+/+}, PDK1^{fl/+}, or PDK1^{fl/-} SDCs were loaded on a SDS-PAGE gel, immunoblotted with anti-phospho-cofilin (S3), anti-cofilin, or anti-Erk1/2 Abs and quantified using a LI-COR Odyssey infrared imaging system. The results are representative of at least three independent experiments. G, analysis of F-actin recovery was performed as described in E, but where indicated cells were resuspended in calcium-free medium (no Ca). H, PDK1^{fl/+} or PDK1^{fl/-} SDC were labeled with Indo-1-AM for 45 min and washed, and calcium flux was measured for 120 s on a LSR FACS machine. After 30 s, 100 ng/ml MIP1 α was added. The results are representative of at least three independent experiments. WT, wild type.

ferent signaling pathways downstream of PDK1 might be affected. The molecular mechanisms involved in the regulation of macropinocytosis by TLRs are still poorly understood. Recently, we showed that activation of either the p38 or the Erk1/2 pathway was required to stimulate enhanced macropinocytosis (18). Therefore, we investigated the phosphorylation of p38 and Erk1/2 in PDK1^{fl/-} SDCs upon LPS stimulation. As shown in Fig. 6A, whereas p38 phosphorylation was not significantly affected, the activation of Erk1/2 was slightly decreased. However, even complete inhibition of Erk1/2 with the mitogen-activated protein kinase/Erk kinase inhibitor PD184352, which potently inhibits Erk1/2 activation, has only a modest effect on TLR enhanced macropinocytosis (18), suggesting that the partial decrease in Erk activation in PDK1^{fl/-} DC is probably not enough to account for the reduced macropinocytosis observed.

It seemed more likely that reduced activity of one or more of the AGC kinases controlled by PDK1 might be responsible for the effects observed. Therefore, we performed a systematic analysis of the activation of several of these kinases in PDK1^{fl/-} DCs. Most PDK1 substrates require prior activation triggered by an extracellular stimulus. We assessed the state of activation of PDK1 downstream effectors upon LPS stimulation by monitoring the phosphorylation of their T-loop. We found that RSK phosphorylation is partially affected, whereas the Akt/PKB phosphorylation is almost completely abolished (Fig. 6, B and C). We also looked at some of the downstream effectors of Akt/PKB, RSK, and S6K. Fig. 6 (B–D) shows that the basal phosphorylation of GSK3 α/β and of S6 is impaired. Taken together, these results indicated that reduced PDK1 activity in DCs resulted in the impaired activation of RSK, PKB, and S6K induced by TLR4 triggering.

PDK1 Overexpression Rescues the Defects in PDK1^{fl/-} DC—Finally, we investigated whether the defects described above could be rescued by reintroducing PDK1, because it was possible that the phenotype arose as an indirect consequence of a lack of PDK1 during mouse development. To restore normal PDK1 levels in PDK1^{fl/-} DC, we infected wild type, PDK1^{fl/+}, or PDK1^{fl/-} BMDC with a retrovirus expressing both PDK1 and GFP (supplemental Fig. S3A). The co-expression of GFP was used

to identify the infected cells by flow cytometry (supplemental Fig. S3B). A retrovirus expressing only GFP was used as a control to rule out any effect caused by the infection itself. The analysis of infected cells showed a substantial increase in PDK1 expression compared with noninfected cells (supplemental Fig. S3C). Importantly, the amount of PDK1 was similar in both PDK1^{fl/+} and PDK1^{fl/-} DC. Because retroviral infection of primary DC is comparatively inefficient (11–24%; supplemental Fig. S3B), we were only able to monitor those parameters that could be measured in GFP-positive cells by flow cytometry.

We first assessed the effect of restored PDK1 expression on the activity of S6K, one of several PDK1 substrates. As shown in Fig. 7A, phosphorylation of the S6K substrate S6 on Ser^{235/236} was enhanced in DC infected with the PDK1 virus, compared with uninfected DC or DC expressing GFP alone. We next

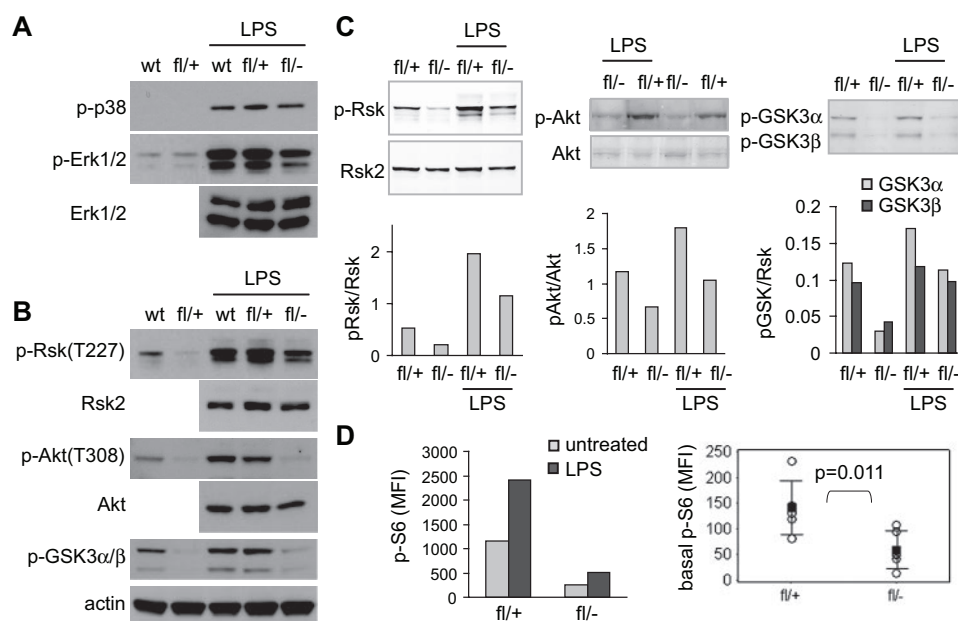


FIGURE 6. Activation of PDK1 substrates is impaired in PDK1^{fl/fl} SDCs. PDK1^{+/+}, PDK1^{+/fl}, or PDK1^{fl/fl} SDC were either untreated or stimulated with 50 ng/ml LPS for 30 min at 37 °C and then lysed. Equal amounts of proteins were resolved on a SDS-PAGE gel. *A* and *B*, cell lysates were immunoblotted with phospho-Erk1/2, phospho-p38, and total Erk1/2 Abs (*A*) or with phospho-RSK S227, phospho-PKB S308, phospho-GSK3α/β S21/9, and total PKB and RSK2 Abs (*B*). Immunoblotting for actin was used as a loading control. *C*, lysates were probed with the same antibodies as in *B* and quantified using a LI-COR Odyssey infrared imaging system. Similar results were obtained with BMDC and are representative of three independent experiments. *D*, *left panel*, PDK1^{fl/+} or PDK1^{fl/fl} SDCs either untreated or stimulated with 50 ng/ml LPS for 30 min were co-stained with anti-CD11c and anti-phospho-S6 Abs and analyzed by flow cytometry. *Right panel*, basal levels of S6 phosphorylation. The *open circles* correspond to one mouse each (*n* = 5 for each genotype). The *black square* represents the mean. The *bars* represents 95% confidence interval. Decreased S6 phosphorylation in PDK1^{fl/fl} DC was significant (*p* = 0.011). *wt*, wild type.

examined the content of F-actin in PDK1 restored and control DC using phalloidin staining. It was not possible to use FITC-DNase I to obtain a G/F-actin ratio because the cells were already expressing GFP. Nonetheless, as judged by phalloidin staining, F-actin levels were clearly enhanced by expression of PDK1 (Fig. 7*B*). This result was obtained in DC from mice of mixed background and in DC from mice backcrossed onto C57/B6. Consistent with a link between PDK1 activity and F-actin-dependent processes, the level of macropinocytosis was also enhanced in DC where the kinase was overexpressed. When stimulated with LPS PDK1^{fl/fl} DC expressing PDK1 showed substantially more dextran uptake compared with the same DC expressing GFP alone (Fig. 7*C*). Interestingly, wild type DC infected with PDK1 virus also showed a similar enhancement, suggesting that PDK1 levels in DC may be limiting even under these conditions. Consistent with that scenario, basal pinocytosis was also stimulated by expression of PDK1 (Fig. 7*C*). This meant that there was little difference in the fold increase in pinocytosis triggered by LPS in PDK1^{fl/fl} DC and in PDK1 rescued PDK1^{fl/fl} DC (data not shown). Again, PDK1 enhanced pinocytosis was seen in both genetic backgrounds. The capacity of reintroduced PDK1 to rescue S6 phosphorylation, elevate F-actin levels, and to enhance both basal and LPS-stimulated macropinocytosis strongly suggests that the phenotype of PDK1^{fl/fl} DC is directly due to low kinase levels and not to indirect factors that affect DC development and differentiation *in vitro*.

DISCUSSION

To initiate immune responses, DCs need to undergo a maturation program typically triggered by the engagement of TLR by microbial products (6). Although TLR downstream signaling pathways have been the focus of intensive research, few reports have studied the role of the Ser/Thr AGC kinase family. In this study, we investigated how the “master kinase” PDK1, which is required to activate the AGC kinases PKB, PKC, PRK1, RSK, S6K, and SGK (7), controlled some aspects of DC function, particularly those triggered by TLR stimulation. Because deletion of the PDK1 gene is embryonic lethal, we used a mouse model in which ~10% of PDK1 is expressed (30). Despite the decrease in PDK1 activity, DC development and homing to lymphoid organs in PDK1^{fl/fl} mice appeared relatively normal. In contrast DCs expanded *in vitro* showed specific abnormalities in their response to TLR stimulation. In particular two different actin-dependent endocytic pathways, macropinocytosis and phagocytosis,

were partially defective in DC from PDK1^{fl/fl} mice. We traced the likely cause of this phenotype to a reduction in actin polymerization rate in these cells. In addition, DCs expanded from spleen showed enhanced production of the cytokines IL-12 and IL-10. Finally, we found that several AGC kinases including PKB, S6K, and RSK that lie downstream of PDK1 were not activated normally in PDK1^{fl/fl} DC.

Our results demonstrating enhanced IL-12 production in PDK1^{fl/fl} SDC are consistent with data indicating that the PI 3-kinase/PKB pathway attenuates inflammatory cytokine production in immune cells. For example, Fukao *et al.* (42) demonstrated enhanced IL-12 production in DCs lacking the p85 regulatory subunit of PI 3-kinase or treated with PI 3-kinase inhibitors. Recent studies identified GSK3β as a potential downstream effector of this response (21, 22) because GSK3β phosphorylation by PKB and its consequent inhibition led to diminished IL-12 production in peripheral blood monocytes. In PDK1^{fl/fl} DC, PKB activation by LPS was impaired boosting GSK3α/β activity, at least as measured by Ser⁹ and Ser²¹ phosphorylation, which would predict the observed enhanced IL-12 production. However, we observed a parallel increase in IL-10 production rather than the reduction observed by Martin *et al.* (21) when GSK3 is kept activated as a result of PI 3-kinase or PKB inhibition. Surprisingly, we observed enhancement of IL-12 and IL-10 production in SDC but not in BMDC. At present we cannot pinpoint the reason for this difference, which

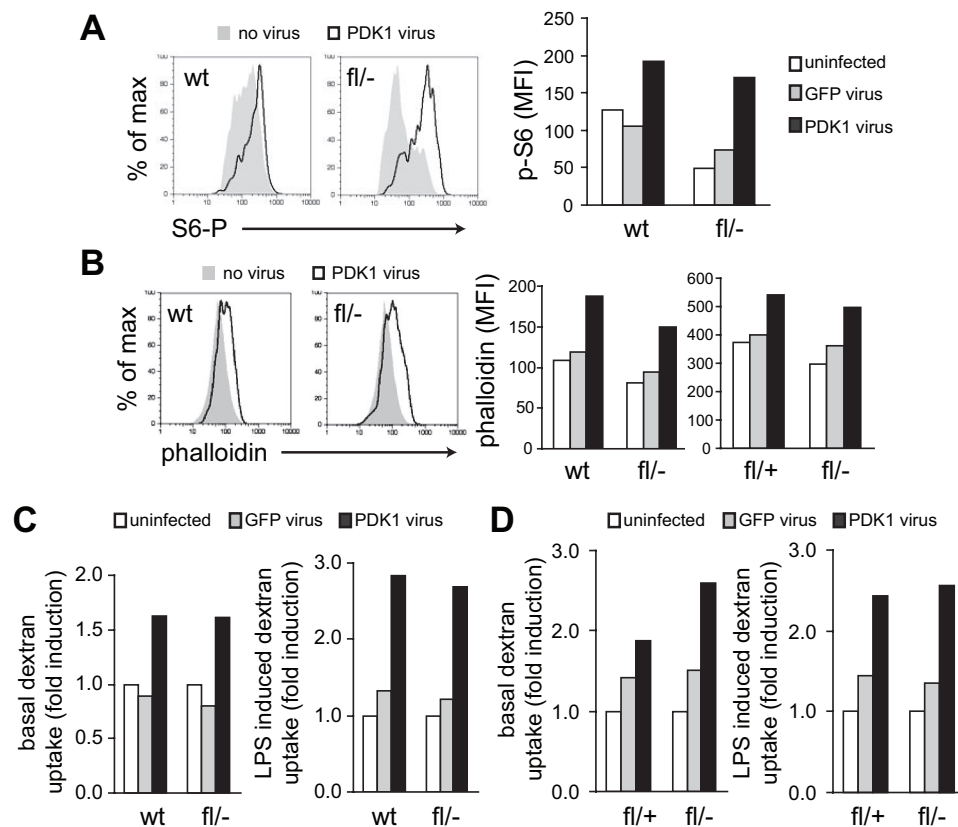


FIGURE 7. Rescue of phenotypic characteristics of PDK1^{fl/-} DC by PDK1 overexpression. A, noninfected or infected BMDC were co-stained with anti-CD11c and anti-phospho-S6 abs and analyzed by flow cytometry. Left panel, overlay histograms showed the S6 phosphorylation levels in noninfected (gray) or PDK1-infected (white) PDK1^{WT} (left histogram) and PDK1^{fl/-} (right histogram) BMDC. Right panel, results showed the median intensity value for one representative experiment of three performed in triplicate. B, PDK1^{+/+}, PDK1^{+/fl}, or PDK1^{fl/-} BMDC either noninfected or infected with GFP virus or PDK1 virus were co-stained with anti-CD11c Ab and phalloidin Alexa-633 and analyzed by flow cytometry. Left panel, overlay histograms showed phalloidin staining in noninfected (gray) or PDK1 infected (white) PDK1^{WT} (left histogram) and PDK1^{fl/-} (right histogram) BMDC. Right panel, results showed the MFI for CD11c⁺ (noninfected) or GFP⁺ CD11c⁺ cells in BMDC from C57/B6 (left histogram) or mixed (right histogram) backgrounds. The results are representative of at least three independent experiments performed in duplicates. C and D, the same cells as in A were untreated or stimulated with 50 ng/ml LPS for 30 min before the addition of Alexa 633-dextran for 10 min and then analyzed by flow cytometry. Pinocytosis (MFI on gated CD11c⁺, GFP⁺ cells) for control (GFP only) and PDK1 virus-infected cells is expressed relative to uninfected cells for basal (left panels) or LPS stimulated (right panels) BMDC from C57/B6 (C) or mixed (D) backgrounds. The results are representative of at least three independent experiments performed in duplicate. wt, wild type.

seems to indicate distinct regulation of cytokine production in different DC types.

One of the striking consequences of low levels of PDK1 activity in DC is a significant reduction in the content of F-actin as well as in its rate of polymerization. Despite this unexpected defect, DC were able to make the various F-actin-rich structures typically observed in DC such as membrane ruffles and podosomes, suggesting that it was their capacity to regulate the polymerization or the depolymerization of F-actin that was affected. A difference in depolymerization rate appeared to be responsible because when external Ca²⁺ was removed (to suppress depolymerization), actin polymerization rates were increased equally for control and PDK1^{fl/-} DC. Moreover, an initial analysis of some of the actin-binding proteins involved in these processes showed that an increased actin depolymerization rate could be due in part to an increase in cofilin activity. Indeed, because cofilin severs actin filaments, this could favor F-actin depolymerization, which in turn will reduce F-actin lev-

els. How could PDK1 affect cofilin phosphorylation levels? Cofilin is inactivated by phosphorylation on Ser³ by LIMK, which in turn is activated by PAK1 (43). Because PAK1 has been reported to be a PDK1 substrate (44), it is possible that in PDK1^{fl/-} DC PAK1 activity is reduced, resulting in an increase in cofilin activity. Inactivation or depletion of cofilin by overexpression of LIMK and antisense strategies, respectively, enhanced phagocytosis (43, 44) consistent with an inverse relationship between cofilin activity and phagocytic activity. Other links between PDK1-activated AGC kinases and actin-driven endo/phagocytosis are also likely to be relevant, however. The most obvious biological consequence of reduced F-actin was a blunted pinocytic and phagocytic response in PDK1^{fl/-} DC. Despite this, presentation of exogenous antigen was actually increased. However, the presentation of antigenic peptides was also enhanced. We found that matured PDK1^{fl/-} DC have increased levels of co-stimulatory molecules, and this apparently more than compensates for any shortfall in antigen uptake.

Several studies have highlighted the crucial role of the PI3K product PtdIns(3,4,5)P₃ during the formation of macropinosomes and phagosomes. This lipid is enriched in the membrane ruffles that give rise to forming macropinosomes and on

the membrane projections that initiate phagocytosis (45–47). Most evidence suggests that PtdIns(3,4,5)P₃ is required for the final stages of pino/phagosome formation (*i.e.* closure). However, the key PH domain bearing proteins that might be recruited to late stage pinosomes/phagosomes are not known. Our results suggest that PDK1 is a possible candidate and may in turn activate effectors such as PKB (which also has a PH domain) that could control the closure stage. Akt/PKB is essential for macropinocytosis in *Dictyostelium* (48) and, working through p70S6 kinase, for optimal phagocytosis in mammalian cells (13). Other evidence implicates p70S6 kinase in actin organization in Swiss 3T3 cells (49).

RSK is another PDK1 substrate that may also be relevant. This kinase has been shown to phosphorylate the actin cross-linker filamin A and the Na⁺/H⁺ transporter NHE1 (50, 51). These two actin-binding proteins act as a scaffold by bringing together actin and actin remodelling proteins. Filamin A acts as a docking site for the Rho GTPases Rac1, cdc42, and RhoA and

their GEFs (e.g. Trio) (52), whereas NHE1 recruits to the plasma membrane the actin polymerization machinery formed by WASP and Arp2/3 through the NIK/Nck complex (49). Earlier work from our own and other labs showed that amiloride, a specific inhibitor of NHE1, blocked macropinocytosis in both epidermal growth factor-stimulated A431 cells (53), and in human dendritic cells (54), and a recent report showed that low levels of PDK1 decreased the activity of the NHE3 transporter in the intestine (55). As part of a larger study of mitogen-activated protein kinase activated kinases in DC responses to TLR ligands, we have recently found that chemical inhibition of RSK blocks the LPS-stimulated pinocytic response (56), supporting the idea that RSK is an important downstream effector of PDK1. However, blockade of RSK does not lead to changes in DC F/G-actin ratio, underlining that several pathways involved in actin regulation are likely to be affected by decreased PDK1 activity. Although deficiencies in AGC kinase activation are likely to underlie the perturbed LPS responses and abnormal F/G-actin ratio in PDK1^{fl/-} DC, we cannot rule out the possibility that other unidentified PDK1 substrates are involved.

Our analysis of the activation status of PDK1 substrates in DC showed that low levels of PDK1 resulted in a significant reduction of the basal or/and LPS activation of RSK, PKB, and S6K. These results were surprising because previous work carried out in the same PDK1^{-/-} mouse model showed that these kinase activities were activated normally after insulin administration in the liver or in skeletal muscle (30). This discrepancy could be due to several factors such as the type of stimuli used, the length of signaling required for activation, and the possibility that DC may simply express less PDK1 than liver cells or skeletal muscle cells. Importantly, we were able to rescue phenotypic characteristics of PDK1^{-/-} DC by reintroducing PDK1. In addition to enhanced levels of S6 protein phosphorylation, PDK1 restored DC showed increased levels of F-actin and enhanced pinocytic activity. Interestingly, introduction of PDK1 stimulated basal levels of pinocytosis and increased F-actin not only in PDK1^{-/-} DC but also in wild type DC. This suggests that PDK1 is limiting in DC for these processes and shows that at least part of the PDK1^{-/-} DC phenotype is directly due to the low levels of this key kinase. It remains possible that there are collateral effects of low PDK1 levels during mouse development, but we have no evidence for this in DC. With a clear role for the AGC kinase family uncovered, it may now be possible to dissect the contribution made by individual family members by establishing DC that express mutant forms of PDK1 that either fail to activate PKB, because of a mutation introduced into the PDK1 PH domain (57) or fail to activate RSK, S6K, and SGK because of a mutation in the PDK1-interacting fragment (PIF pocket) (58) that prevents interaction with these targets. Both PDK1 mutations are embryonic lethal, but DC might be established from appropriate embryonic stem cells (59) or by *in vitro* deletion of a floxed wild type allele expressed alongside the mutated PDK1 allele.

Acknowledgments—We thank D. Alessi and colleagues for PDK1^{-/-} mice and H. Hinton and D. Cantrell for cryopreserved PDK1^{-/-} bone marrow and helpful suggestions. We thank H. Svensson for advice on the phagocytosis assays.

REFERENCES

- Banchereau, J., and Steinman, R. M. (1998) *Nature* **392**, 245–252
- Banchereau, J., Briere, F., Caux, C., Davoust, J., Lebecque, S., Liu, Y. J., Pulendran, B., and Palucka, K. (2000) *Annu. Rev. Immunol.* **18**, 767–811
- Trombetta, E. S., and Mellman, I. (2005) *Annu. Rev. Immunol.* **23**, 975–1028
- Reis e Sousa, C. (2006) *Nat. Rev. Immunol.* **6**, 476–483
- O'Neill, L. A. (2006) *Curr. Opin. Immunol.* **18**, 3–9
- Akira, S., and Takeda, K. (2004) *Nat. Rev. Immunol.* **4**, 499–511
- Mora, A., Komander, D., van Aalten, D. M., and Alessi, D. R. (2004) *Semin. Cell Dev. Biol.* **15**, 161–170
- Vanhaesebroeck, B., and Alessi, D. R. (2000) *Biochem. J.* **346**, 561–576
- Larsen, E. C., DiGennaro, J. A., Saito, N., Mehta, S., Loegering, D. J., Mazurkiewicz, J. E., and Lennartz, M. R. (2000) *J. Immunol.* **165**, 2809–2817
- Larsson, C. (2006) *Cell Signal.* **18**, 276–284
- Swanson, J. A., and Hoppe, A. D. (2004) *J. Leukocyte Biol.* **76**, 1093–1103
- Cantrell, D. (2002) *Semin. Immunol.* **14**, 19–26
- Ganesan, L. P., Wei, G., Pengal, R. A., Moldovan, L., Moldovan, N., Ostrowski, M. C., and Tridandapani, S. (2004) *J. Biol. Chem.* **279**, 54416–54425
- Aksoy, E., Goldman, M., and Willems, F. (2004) *Int. J. Biochem. Cell Biol.* **36**, 183–188
- Tan, S. L., and Parker, P. J. (2003) *Biochem. J.* **376**, 545–552
- Burns, S., Hardy, S. J., Buddle, J., Yong, K. L., Jones, G. E., and Thrasher, A. J. (2004) *Cell Motil. Cytoskeleton* **57**, 118–132
- Blander, J. M., and Medzhitov, R. (2004) *Science* **304**, 1014–1018
- West, M. A., Wallin, R. P., Matthews, S. P., Svensson, H. G., Zaru, R., Ljunggren, H. G., Prescott, A. R., and Watts, C. (2004) *Science* **305**, 1153–1157
- West, M. A., Prescott, A. R., Eskelinen, E. L., Ridley, A. J., and Watts, C. (2000) *Curr. Biol.* **10**, 839–848
- Aksoy, E., Amraoui, Z., Goriely, S., Goldman, M., and Willems, F. (2002) *Eur. J. Immunol.* **32**, 3040–3049
- Martin, M., Rehani, K., Jope, R. S., and Michalek, S. M. (2005) *Nat. Immunol.* **6**, 777–784
- Rodionova, E., Conzelmann, M., Maraskovsky, E., Hess, M., Kirsch, M., Giese, T., Ho, A. D., Zoller, M., Dreger, P., and Luft, T. (2006) *Blood* **109**, 1584–1592
- Newton, A. C. (2003) *Biochem. J.* **370**, 361–371
- Biondi, R. M., Komander, D., Thomas, C. C., Lizcano, J. M., Deak, M., Alessi, D. R., and van Aalten, D. M. (2002) *EMBO J.* **21**, 4219–4228
- Komander, D., Fairservice, A., Deak, M., Kular, G. S., Prescott, A. R., Peter Downes, C., Safrany, S. T., Alessi, D. R., and van Aalten, D. M. (2004) *EMBO J.* **23**, 3918–3928
- Sarbasov, D. D., Guertin, D. A., Ali, S. M., and Sabatini, D. M. (2005) *Science* **307**, 1098–1101
- Frodin, M., Jensen, C. J., Merienne, K., and Gammeltoft, S. (2000) *EMBO J.* **19**, 2924–2934
- Balendran, A., Biondi, R. M., Cheung, P. C., Casamayor, A., Deak, M., and Alessi, D. R. (2000) *J. Biol. Chem.* **275**, 20806–20813
- Balendran, A., Hare, G. R., Kieloch, A., Williams, M. R., and Alessi, D. R. (2000) *FEBS Lett.* **484**, 217–223
- Lawlor, M. A., Mora, A., Ashby, P. R., Williams, M. R., Murray-Tait, V., Malone, L., Prescott, A. R., Lucocq, J. M., and Alessi, D. R. (2002) *EMBO J.* **21**, 3728–3738
- Mora, A., Lipina, C., Tronche, F., Sutherland, C., and Alessi, D. R. (2005) *Biochem. J.* **385**, 639–648
- Mora, A., Sakamoto, K., McManus, E. J., and Alessi, D. R. (2005) *FEBS Lett.* **579**, 3632–3638
- Hinton, H. J., Alessi, D. R., and Cantrell, D. A. (2004) *Nat. Immunol.* **5**, 539–545
- Nirula, A., Ho, M., Phee, H., Roose, J., and Weiss, A. (2006) *J. Exp. Med.* **203**, 1733–1744
- Moss, C. X., Matthews, S. P., Lamond, D. J., and Watts, C. (2005) *J. Biol. Chem.* **280**, 18498–18503
- Shortman, K., and Liu, Y. J. (2002) *Nat. Rev. Immunol.* **2**, 151–161

37. Villadangos, J. A., and Heath, W. R. (2005) *Semin. Immunol.* **17**, 262–272
38. Takenawa, T., and Suetsugu, S. (2007) *Nat. Rev. Mol. Cell. Biol.* **8**, 37–48
39. Goley, E. D., and Welch, M. D. (2006) *Nat. Rev. Mol. Cell. Biol.* **7**, 713–726
40. Arber, S., Barbayannis, F. A., Hanser, H., Schneider, C., Stanyon, C. A., Bernard, O., and Caroni, P. (1998) *Nature* **393**, 805–809
41. Ono, S. (2007) *Int. Rev. Cytol.* **258**, 1–82
42. Fukao, T., Tanabe, M., Terauchi, Y., Ota, T., Matsuda, S., Asano, T., Kadowaki, T., Takeuchi, T., and Koyasu, S. (2002) *Nat. Immunol.* **3**, 875–881
43. Edwards, D. C., Sanders, L. C., Bokoch, G. M., and Gill, G. N. (1999) *Nat. Cell Biol.* **1**, 253–259
44. King, C. C., Gardiner, E. M., Zenke, F. T., Bohl, B. P., Newton, A. C., Hemmings, B. A., and Bokoch, G. M. (2000) *J. Biol. Chem.* **275**, 41201–41209
45. Marshall, J. G., Booth, J. W., Stambolic, V., Mak, T., Balla, T., Schreiber, A. D., Meyer, T., and Grinstein, S. (2001) *J. Cell Biol.* **153**, 1369–1380
46. Dormann, D., Weijer, G., Dowler, S., and Weijer, C. J. (2004) *J. Cell Sci.* **117**, 6497–6509
47. Araki, N., Johnson, M. T., and Swanson, J. A. (1996) *J. Cell Biol.* **135**, 1249–1260
48. Rupper, A., Lee, K., Knecht, D., and Cardelli, J. (2001) *Mol. Biol. Cell* **12**, 2813–2824
49. Putney, L. K., Denker, S. P., and Barber, D. L. (2002) *Annu. Rev. Pharmacol. Toxicol.* **42**, 527–552
50. Tigges, U., Koch, B., Wissing, J., Jockusch, B. M., and Ziegler, W. H. (2003) *J. Biol. Chem.* **278**, 23561–23569
51. Woo, M. S., Ohta, Y., Rabinovitz, L., Stossel, T. P., and Blenis, J. (2004) *Mol. Cell. Biol.* **24**, 3025–3035
52. Stossel, T. P., Condeelis, J., Cooley, L., Hartwig, J. H., Noegel, A., Schleicher, M., and Shapiro, S. S. (2001) *Nat. Rev. Mol. Cell. Biol.* **2**, 138–145
53. West, M. A., Bretscher, M. S., and Watts, C. (1989) *J. Cell Biol.* **109**, 2731–2739
54. Sallusto, F., Cella, M., Danieli, C., and Lanzavecchia, A. (1995) *J. Exp. Med.* **182**, 389–400
55. Sandu, C., Artunc, F., Palmada, M., Rexhepaj, R., Grahammer, F., Hussain, A., Yun, C., Alessi, D. R., and Lang, F. (2006) *Am. J. Physiol.* **291**, G868–G876
56. Zaru, R., Ronkina, N., Gaestel, M., Arthur, J. S. C., and Watts, C. (2007) *Nat. Immunol.* **8**, 1227–1235
57. McManus, E. J., Collins, B. J., Ashby, P. R., Prescott, A. R., Murray-Tait, V., Armit, L. J., Arthur, J. S., and Alessi, D. R. (2004) *EMBO J.* **23**, 2071–2082
58. Collins, B. J., Deak, M., Arthur, J. S., Armit, L. J., and Alessi, D. R. (2003) *EMBO J.* **22**, 4202–4211
59. Fairchild, P. J., Brook, F. A., Gardner, R. L., Graca, L., Strong, V., Tone, Y., Tone, M., Nolan, K. F., and Waldmann, H. (2000) *Curr. Biol.* **10**, 1515–1518

3-Phosphoinositide-dependent Kinase 1 Deficiency Perturbs Toll-like Receptor Signaling Events and Actin Cytoskeleton Dynamics in Dendritic Cells

Rossana Zaru, Pamela Mollahan and Colin Watts

J. Biol. Chem. 2008, 283:929-939.

doi: 10.1074/jbc.M708069200 originally published online November 8, 2007

Access the most updated version of this article at doi: [10.1074/jbc.M708069200](https://doi.org/10.1074/jbc.M708069200)

Alerts:

- [When this article is cited](#)
- [When a correction for this article is posted](#)

[Click here](#) to choose from all of JBC's e-mail alerts

Supplemental material:

<http://www.jbc.org/content/suppl/2007/11/08/M708069200.DC1>

This article cites 59 references, 25 of which can be accessed free at

<http://www.jbc.org/content/283/2/929.full.html#ref-list-1>